

RESEARCH

Open Access



# Inhibition of ABCC9 by zinc oxide nanoparticles induces ferroptosis and inhibits progression, attenuates doxorubicin resistance in breast cancer

Yang Li<sup>1</sup>, Cui Jiang<sup>2</sup>, Xiaoxue Zhang<sup>3</sup>, Zhixuan Liao<sup>1</sup>, Long Chen<sup>1</sup>, Shuang Li<sup>1</sup>, Shunxiong Tang<sup>4</sup>, Zhe Fan<sup>5</sup> and Qiang Zhang<sup>1\*</sup>

\*Correspondence:

qiangsuzhanrgfrz@163.com

<sup>1</sup> Department of Breast Surgery, Cancer Hospital of China Medical University, Liaoning Cancer Hospital & Institute, No. 44 Xiaoheyan Road, Dadong District, Shenyang 110042, Liaoning Province, People's Republic of China

Full list of author information is available at the end of the article

## Abstract

**Background:** Zinc oxide nanoparticles (ZONs) are a type of nanomaterial that has presented anti-cancer properties in breast cancer (BC). However, the function of ABCC9 in BC and its correlation with ZONs are still elusive.

**Methods:** Here, we identified the crucial role of ABCC9 in modulating ferroptosis and doxorubicin (Dox) resistance in BC and the targeted function of ZONs to ABCC9.

**Results:** The silencing of ABCC9 significantly repressed the viability of BC cells. The knockdown of ABCC9 decreased the numbers of Edu-positive BC cells. Conversely, BC cell apoptosis was increased by the inhibition of ABCC9. Besides, the silencing of ABCC9 reduced the capability of migration and invasion of BC cells. Significantly, tumorigenicity analysis demonstrated that the tumor growth of BC cells was suppressed by the depletion of ABCC9 in the xenograft model of nude mice. Moreover, the treatment of ferroptosis activator erastin repressed cell viability of BC cells and ABCC9 overexpression rescued the repression. Similarly, the numbers of Edu-positive BC cells were inhibited by erastin and the overexpression of ABCC9 reversed the inhibitory effect of erastin. The levels of GSH were decreased and MDA, lipid ROS, and iron levels were increased by the treatment of erastin, while the ABCC9 overexpression could reverse these results in BC cells. Consistently, erastin suppressed the expression of ferroptosis inhibitory factors, including GPX4 and SLC7A11, in BC cells and the overexpression of ABCC9 rescued the expression. The IC50 value of Dox was reduced by the knockdown of ABCC9 in Dox-resistant BC cells (BC/Dox). The numbers of Edu-positive BC/Dox cells were attenuated by the depletion of ABCC9. Meanwhile, the apoptosis of BC/Dox cells was stimulated by the silencing of ABCC9. Furthermore, the treatment of ZONs attenuated Dox resistance of BC cells. ZONs remarkably repressed the expression of ABCC9 in BC/Dox cells. ZONs inhibited the cell viability of BC/Dox cells and the overexpression of ABCC9 reversed the repression. Moreover, the treatment of ZONs reduced GSH levels and enhanced MDA, lipid ROS, and iron levels in erastin-stimulated BC/Dox cells.

**Conclusions:** In conclusion, we discovered that the inhibition of ABCC9 by zinc oxide nanoparticles induces ferroptosis and attenuates Dox resistance in BC.



**Keywords:** Breast cancer, Ferroptosis, Doxorubicin resistance, ABCC9, Zinc oxide nanoparticles

## Background

Breast cancer (BC) is a typical gynecological cancer that holds the top incidence and mortality among women in both developed and developing countries (Siegel et al. 2020). Even though the greatly developed medical therapeutic approaches, including surgery, targeted therapies, and chemo- and radio-therapy, have dramatically improved the prognosis and life quality of BC patients, the drug resistance remains a huge impediment for the cure of BC (Harbeck and Gnant 2017). Drug resistance could lead to suppressed therapeutic response and cancer recurrence (McGranahan and Swanton 2017). Doxorubicin (Dox) is one of the most widely applied chemotherapy drugs in cancers, including BC, and it has been approved that Dox resistance usually suggests treatment failure (Telli et al. 2019). The generation of Dox-resistance is complicated. Studies indicated that cancer cells growing in the hypoxic environments are resistant to Dox treatment which is caused by weakened production of intracellular ROS (Wouters et al. 2007; Karagoz et al. 2008). And the increase of local oxygen could notably elevate the cytotoxicity of Dox by increasing the generation of ROS, and ultimately alleviating the resistance of solid malignancies to DOX (Huang et al. 2016). Besides, p53 mutations play an important role in cancer cell resistance to chemotherapeutic drugs.

Mechanistically, drug resistance is closely related with drug transporters, typically the ATP-binding cassette (ABC) family members, which manipulate drug efflux and determine the drug delivery efficacy into cancer cell (Dallavalle et al. 2020). Several ABC transporters such as ABCB1, ABCG2, and ABCC1 (MRP1) has been reported as a regulator of multidrug resistance (MDR) (Kathawala et al. 2015; Li et al. 2016). Another ABC protein, ABCC9, was involved in Daple/ $\beta$ -catenin signaling mediated cisplatin-resistance in nasopharyngeal carcinoma (Zhang et al. 2020a, b). It has been recently indicated that ABCC9 is elevated in the clinical triple-negative breast cancer samples and serves as a potential diagnostic biomarker for triple-negative breast cancer patients (Zhang et al. 2020a, b). However, the function of ABCC9 in triple-negative breast cancer remains unclear. Accordingly, we aimed to explore the effect of ABCC9 on the progression of triple-negative breast cancer.

Ferroptosis is a recently spotted non-apoptotic regulated cell death promoted by iron-dependent lipid peroxidation (Dixon et al. 2012). It differs from other classic cell death manners, such as necrosis, autophagy and apoptosis, in various aspects, including biochemistry, morphology and genetics (Dixon et al. 2012). When ferroptosis occurred, free iron and lipid peroxides increased in cell, which subsequently caused the accumulation of intracellular reactive oxygen species (ROS) and the following oxidative cell death (Yagoda et al. 2007). It has been revealed that ferroptosis caused by small molecules notably inhibited tumor growth and increased sensitized cancer cell response to chemotherapy (Lu et al. 2017). Moreover, induction of ferroptosis in cancer stem cells facilitates better therapeutic outcomes of chemotherapy (Elgendy et al. 2020). Therefore, targeting ferroptosis has been regarded as a promising therapeutic strategy for drug resistance.

Zinc oxide nanoparticles (ZONs) are a type of nanomaterial that has been used in industrial products including coating and paint (Steele et al. 2009). Scientific research

demonstrated potential therapeutic activity of ZONs and its role as a drug delivery system (Hu and Du 2020). ZONs are capable of targeting multiple cancer cell types such as cancer cells and cancer stem cells, and participates in various cellular functions including proliferation, metastasis, immunosurveillance, as well as drug sensitivity (Hu and Du 2020; Ruenraroengsak et al. 2019). ZONs could load and release Dox in tumor sites responding to the acidic environment, which facilitates the penetration and toxicity of Dox (Liu et al. 2016). Moreover, as a cytotoxic agent, ZONs exhibited high efficacy to target drug-resistant cancer cells (Wang et al. 2017). Nevertheless, the detailed mechanisms involved in ZONs-mediated sensitizing of cancer cells to Dox are largely unknown.

In this work, we suggested that ZONs induced ferroptosis in breast cancer cells and regulated resistance to Dox, through suppressing ABCC9 function. Our work presented new evidence for ZONs as a promising therapeutic manner for BC, especially the drug resistant patients.

## **Materials and methods**

### **Materials**

ZONs were obtained from Alfa Aesar Chemical (China). Dox and erastin were purchased from Sigma. The shRNAs targeting ABCC9 (shABCC9) and p53 (shP53), pcDNA-ABCC9 vectors overexpressing ABCC9 (short as ABCC9 OE), and the corresponding negative controls (NCs) were designed and synthesized by QIAGEN (Germany). Lipofectamine 2000 was purchased from Invitrogen and used for cell transfection following manufacturer's protocol.

### **Patients and tissue samples**

We included 152 patients, who received surgical operation in our hospital. The patients are divided into two groups (ABCC9-high and ABCC9-low) according to the relative expression of ABCC9. Tumor tissues were collected during operation and subjected to real-time PCR to evaluate the level of ABCC9. All experiments have acquired the consent of patients and were performed under approval of Cancer Hospital of China Medical University.

### **Cell lines and treatment**

Breast cancer cell line MDA-MB-231 and MDA-MB-468 were obtained from American Type Culture Collection (ATCC, USA). The Dox-resistant cells (MDA-MB-231/DOX and MDA-MB-468/DOX) were established by constant exposure to Dox with elevated doses (0.2 µg/mL to 5 µg/mL) over 10 months. All cells were cultured in Dulbecco's modified Eagle's medium (DMEM, Hyclone, USA) supplemented with 10% FBS (Gibco, USA) and 1% penicillin and streptomycin mixture (Solarbio, China), in a humidified 37 °C incubator filled with 5% CO<sub>2</sub>. For in vitro study, BC cells were treated with Dox (0, 0.5, 1, 1.5, 2 µg/mL), Erastin (5 µM), ferrostatin (1 mmol/L) and/or ZONs (30 µg/mL) for 24 h.

### Cell proliferation and apoptosis

Parental or Dox-resistant BC cells were treated with as indicated in each experiment, then subjected to cell counting kit 8 (CCK-8, Solarbio) and 5-ethynyl-2'-deoxyuridine (Edu) assay (Thermo) to determine cell proliferation, and flow cytometry to measure cell apoptosis. For CCK-8 experiments, cells were seeded in 96-well plates (5000 cells per well) after treatment, and cultured for 24, 48, 72, and 96 h. The CCK-8 reagent (10  $\mu$ L) was added into each well and incubated for 2 h. The optical density at 450 nm was measured by a microplate reader (Thermo).

For Edu assay, cells were fixed, permeabilized, then incubated with Edu (50  $\mu$ M) for 3 h, followed by nuclei staining with DAPI (1  $\mu$ g/mL, Sigma) for 10 min. The Edu-positive cells were photographed under a fluorescence microscopy (Carl Zeiss, Germany).

For cell apoptosis detection, the apoptotic cells were stained with an FITC-Annexin V/PI detection kit (Beyotime, China). In brief, cells were harvested, washed with PBS, then stained with FITC-Annexin V (5  $\mu$ L) and PI (5  $\mu$ L) for 10 min, respectively. The samples were then detected in a flow cytometry (BD Biosciences, USA).

### Transwell assay

The treated cells were collected, resuspended in serum-free DMEM, and seeded in upper chamber of transwell plate (Corning). Complete medium containing FBS (10%) was added in lower chamber. To evaluate the cell invasion, the upper chamber was coated with Matrigel (BD Biosciences). The cells were incubated for 24 h, then fixed with 4% paraformaldehyde (PFA) and stained with 0.5% crystal violet for 10 min. The invaded and migrated cells were photographed and counted with 5 random areas.

### Quantitative real-time PCR (qPCR) assay

The RNA was extracted from BC cells by using TriZol reagent (Thermo) after treatment, reverse transcribed to cDNA by using Super Script III kit (Invitrogen). Subsequently, the relative level of ABCC9 was quantified by SYBR Premix kit (Takara, Japan), and normalized to GAPDH. The results were calculated with  $2^{-\Delta\Delta C_t}$  method. All primers were obtained from RiboBio (China):

ABCC9: forward primer, 5'-TCAACCTGGTCCCTCATGTCT-3'; reverse primer, 5'-CAGGAGAGCGAATGTAAGAATCC-3';

GAPDH: forward primer, 5'-ACAACCTTGGTATCGTGGAAGG-3'; reverse primer, 5'-GCCATCACGCCACAGTTTC-3'.

### Western blotting

Protein extracts of BC cells were obtained by using RIPA lysis buffer (Beyotime), and subjected to SDS-PAGE and blotting to NC membranes. The blots were probed with primary antibodies including anti-ABCC9 (1:2000, Abcam, USA), anti-GPX4 (1:1000, Abcam), anti-SLC7A11 (1:1000, Abcam), anti-p53 (1:1000, Abcam), anti-caspase3 (1:1000, Abcam, USA), anti-cleaved caspase3 (1:1000, Abcam, USA), anti-caspase9 (1:1000, Abcam, USA), anti-cleaved caspase9 (1:1000, Abcam, USA), anti- $\beta$ -actin (1:1000, Abcam). Secondary HRP-conjugated anti-mouse or anti-rabbit antibodies and ECL solution were adopted for detection and visualization in a Gel Image system (GE, USA).

### Detection of ferroptosis

Cell apoptosis was evaluated by detection of malondialdehyde (MDA), glutathione (GSH), lipid ROS and iron levels. Commercial detection kits including MDA assay kit, GSH assay kit, C11-BODIPY probe, and Iron Assay Kit were purchased from Thermo, and used in accordance with the manufacturer's instructions.

### Xenograft model and immuno-histological chemistry (IHC)

Female SCID/nude mice aged 6 weeks were purchased from Charles River Laboratories (China) and randomly divided into experimental groups ( $n=5$  for each group). All experiments were conducted under the guidance and authorization of Laboratory Animal Management Committee of Cancer Hospital of China Medical University. For in vivo mice model, MDA-MB-231 cells transfected with shABCC9 or MDA-MB-231/Dox cells transfected with ABCC9 OE ( $1 \times 10^6$  per site) were suspended in saline (100  $\mu$ L), and subcutaneously injected into the right flanks of nude mice (6-week-old). The mice in control group were injected with saline. For treatment, ZONs (2 mg/kg) were subcutaneously injected into tumor sites every 2 days, when the tumor volume reached 100 mm<sup>3</sup>. Tumor size was measured every 3 days, and calculated by the following equation: length  $\times$  (width)<sup>2</sup>/2. At last, the mice were killed 25 days after inoculation of tumors, and the tumors were collected, photographed and weighed. To conduct ki67 staining, the collected tumors were fixed, paraffin-embedded, made into 5- $\mu$ m-thick slices. The slices were subjected to standard IHC procedures, and probed by ki67 antibody (1:100 Abcam). Five random fields of staining were photographed.

### Characterization of ZON nanoparticles

The synthesized ZON were characterized by UV-VIS spectroscopy (AQ8000, Thermo, USA), Fourier transform infra-red (FTIR) spectroscopy, and scanning electron microscopy (SEM). The optical properties of ZON were checked at various wavelengths ranged from 200 to 800 nm. The functional group of nanoparticles were observed by FTIR. The morphology and size of the nanoparticles were evaluated by SEM.

### Statistical analysis

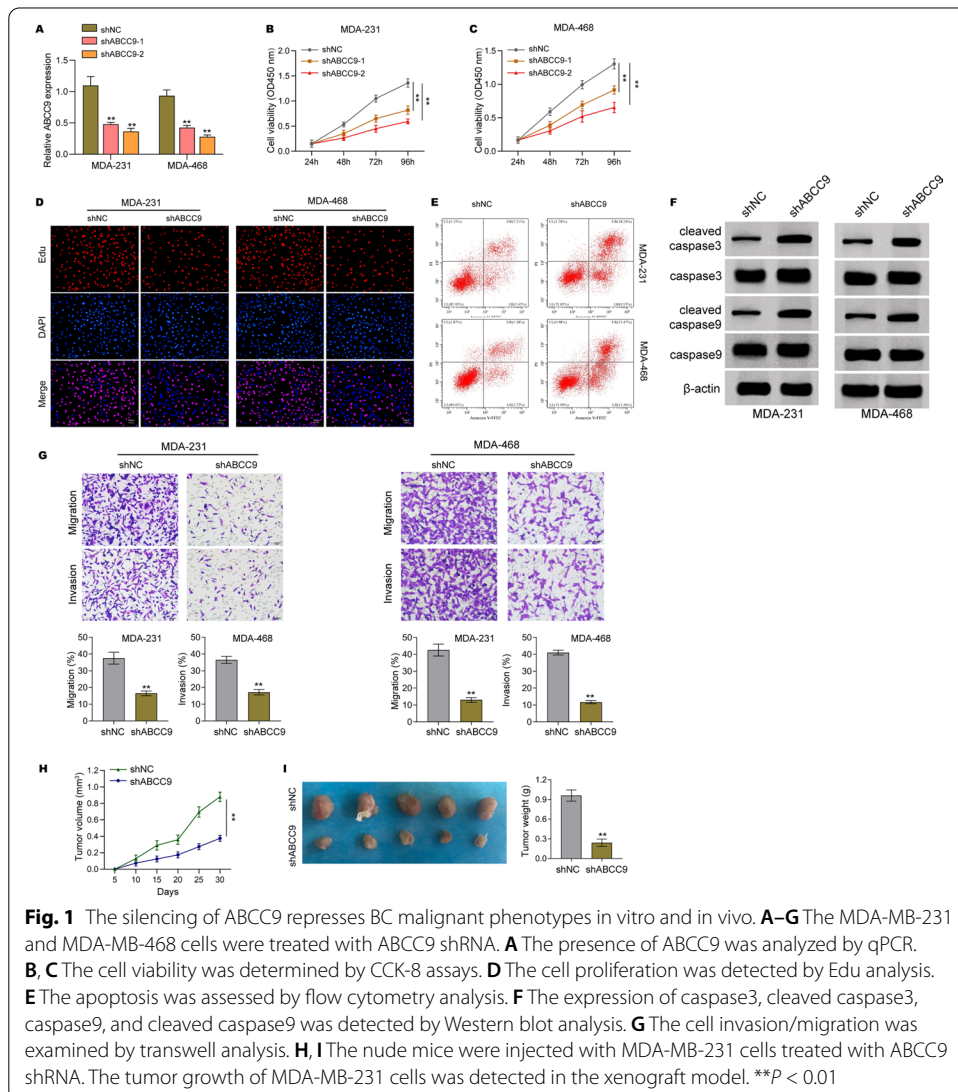
SPSS 22.0 software was used for analysis of the data. Data were shown as means  $\pm$  SD. The statistical differences between two or more groups were evaluated by Student's *t*-test or one-way ANOVA, and were considered to be statistically significant with  $p < 0.05$ .

## Results

### The silencing of ABCC9 represses BC malignant phenotypes in vitro and in vivo

We initially validated that the expression of ABCC9 was elevated in the clinical BC tissues ( $n=152$ ) and the high expression of ABCC9 was associated with the poor survival of BC patients (Additional file 1: Fig. S1A and B). Given that the function of ABCC9 in BC cells was unreported, we assessed the effect of ABCC9 on the malignant phenotypes of BC cells. We first determined the level of ABCC9 in different breast cancer cell lines, including the ER-positive cell line MCF-7 and T47D,

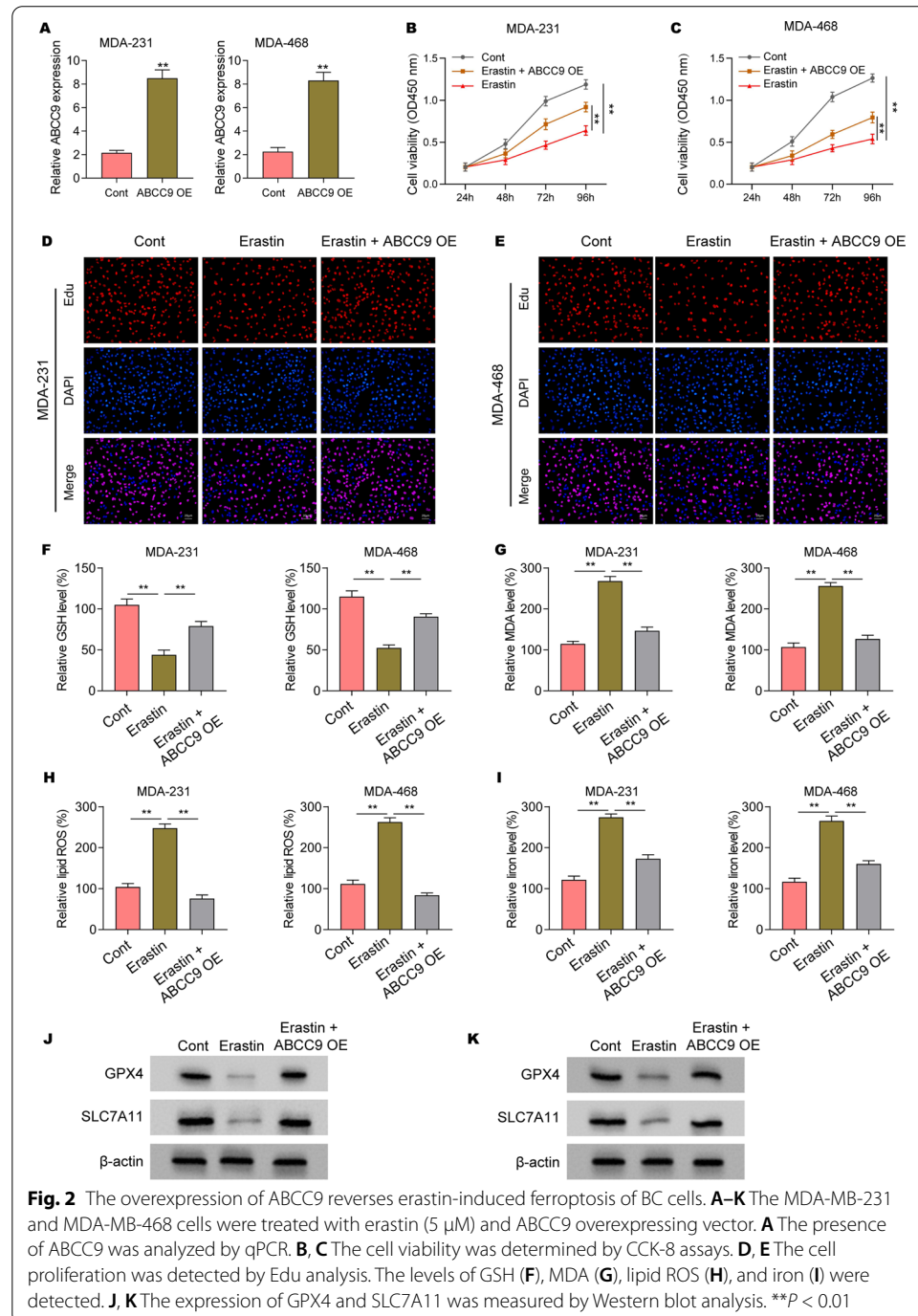
HER2-positive cell line SKBR-3, and triple-negative cell line MDA-MB-231 and MDA-MB-468. The MDA-MB-231 and MDA-MB-468 exhibited highest levels of ABCC9, hence were chosen for subsequent experiments (Additional file 2: Fig. S2). The efficiency of ABCC9 depletion by shRNAs was verified in the MDA-MB-231 and MDA-MB-468 cells (Fig. 1A). Meanwhile, the silencing of ABCC9 by shRNAs significantly repressed the viability of MDA-MB-231 and MDA-MB-468 cells (Fig. 1B and C), in which ABCC9 shRNA-2 showed a higher effect and was selected in the application of subsequent analysis. Obviously, the knockdown of ABCC9 decreased the numbers of Edu-positive MDA-MB-231 and MDA-MB-468 cells (Fig. 1D). Conversely, MDA-MB-231 and MDA-MB-468 cell apoptosis was increased by the inhibition of ABCC9 (Fig. 1E). Consistently, the expression of cleaved caspase3 and cleaved caspase 9 was induced by the depletion of ABCC9 in the cells (Fig. 1F). Moreover, the silencing of ABCC9 reduced the capability of migration and invasion of MDA-MB-231 and MDA-MB-468 cells (Fig. 1G). Significantly, tumorigenicity analysis demonstrated that the



tumor growth of MDA-MB-231 cells was suppressed by the depletion of ABCC9 in the xenograft model of nude mice (Fig. 1H and I). Collectively, these results show that the silencing of ABCC9 represses BC malignant phenotypes in vitro and in vivo.

### The overexpression of ABCC9 reverses erastin-induced ferroptosis of BC cells

Next, we were interested in the impact of ABCC9 on BC cell ferroptosis. The overexpression of ABCC9 was validated in MDA-MB-231 and MDA-MB-468 cells (Fig. 2A).

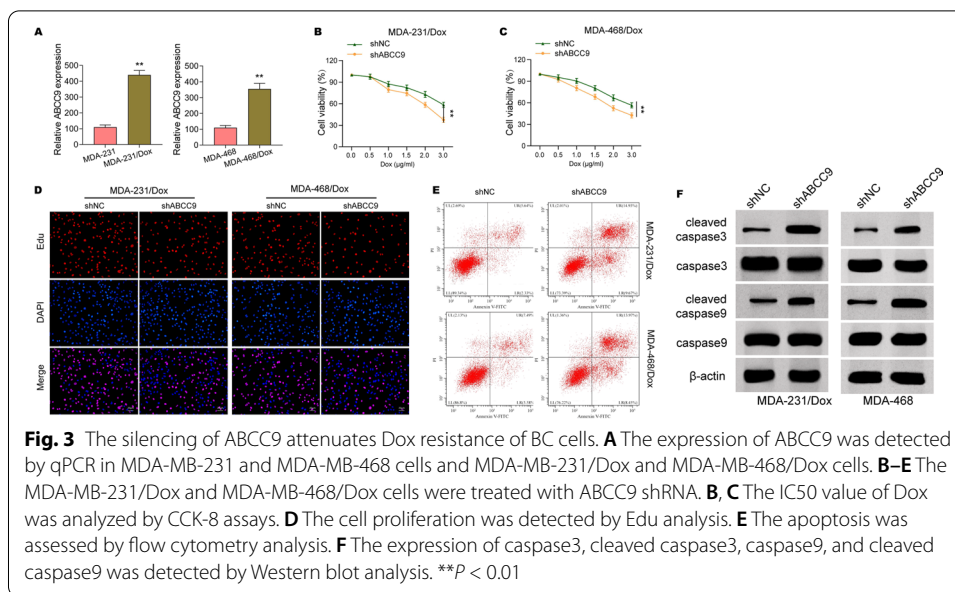


Significantly, the treatment of ferroptosis activator erastin repressed cell viability of MDA-MB-231 and MDA-MB-468 cells and ABCC9 overexpression rescued the repression in the cells (Fig. 2B and C). Similarly, the numbers of Edu-positive MDA-MB-231 and MDA-MB-468 cells were inhibited by erastin and the overexpression of ABCC9 reversed the inhibitory effect of erastin (Fig. 2D and E). The levels of GSH were decreased and MDA, lipid ROS, and iron levels were increased by the treatment of erastin, while the ABCC9 overexpression could reverse this results in MDA-MB-231 and MDA-MB-468 cells (Fig. 2F–I). Consistently, erastin suppressed the expression of ferroptosis inhibitory factors, including GPX4 and SLC7A11, in MDA-MB-231 and MDA-MB-468 cells and the overexpression of ABCC9 rescued the expression (Fig. 2J and K), suggesting that overexpression of ABCC9 reverses erastin-induced ferroptosis of BC cells.

Moreover, we validated that the depletion of ABCC9 inhibited cell viability of MDA-MB-231 and MDA-MB-468 cells and ferroptosis inhibitor ferrostatin-1 (Fer-1) rescued the repression in the cells (Additional file 3: Fig. S3A). Similarly, the numbers of Edu-positive MDA-MB-231 and MDA-MB-468 cells were repressed by ABCC9 knockdown and Fer-1 reversed the inhibitory effect (Additional file 3: Fig. S3B). The levels of GSH were decreased and MDA, lipid ROS, and iron levels were increased by the silencing of ABCC9, while Fer-1 could reverse this results in MDA-MB-231 and MDA-MB-468 cells (Additional file 3: Fig. S3C–F). Consistently, ABCC9 depletion suppressed the expression of ferroptosis inhibitory factors, including GPX4 and SLC7A11, in MDA-MB-231 and MDA-MB-468 cells and Fer-1 rescued the expression (Additional file 3: Fig. S3G).

#### **The silencing of ABCC9 attenuates Dox resistance of BC cells**

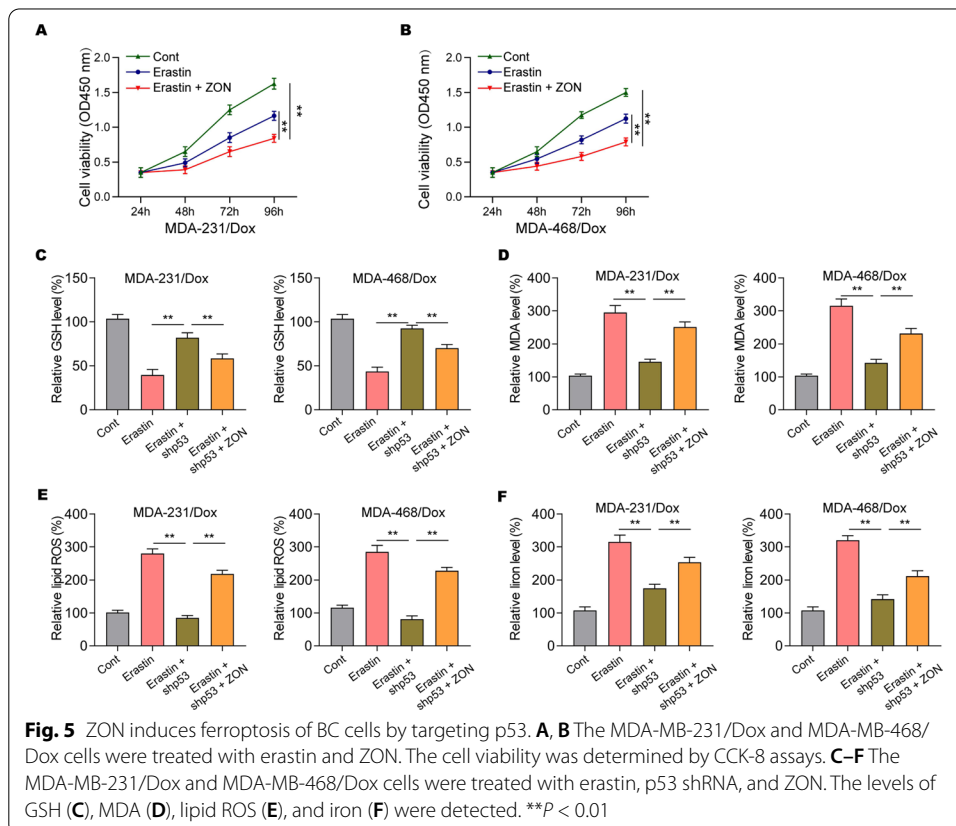
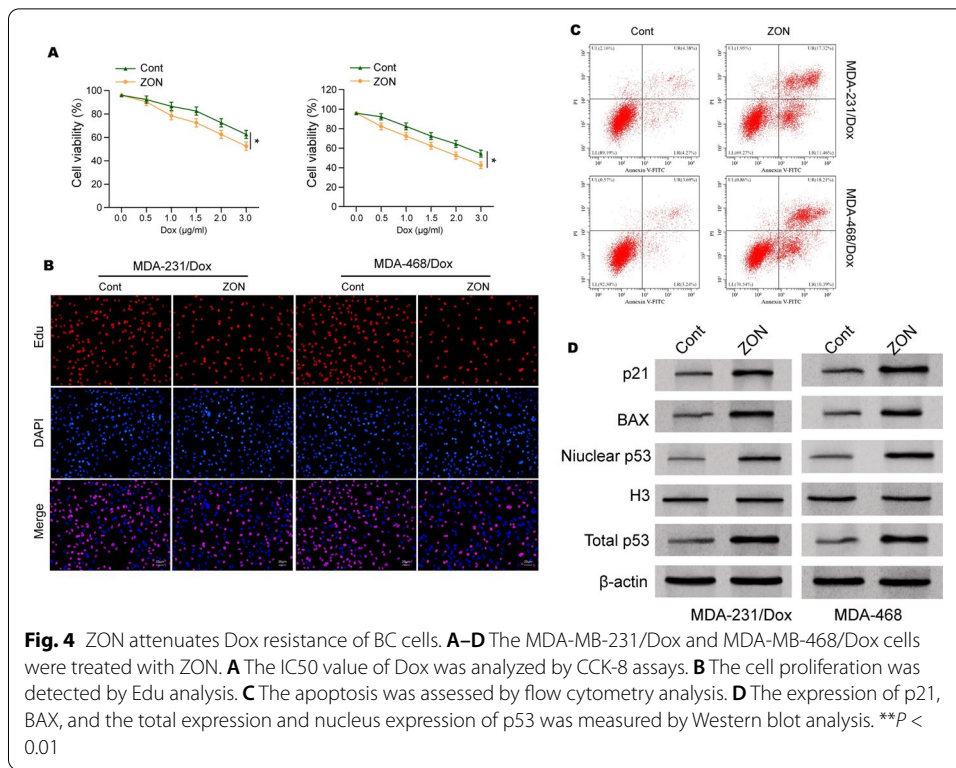
Then, we are concerned about the function of ABCC9 in the modulation of Dox resistance of BC cells. We established Dox-resistant MDA-MB-231 (MDA-MB-231/Dox) and MDA-MB-468 (MDA-MB-468/Dox) cells by constant treatment with Dox for 10 months. The successful establishment of MDA-MB-231/Dox and MDA-MB-468/Dox was validated by higher cell viability (Additional file 4: Fig. S4A) and proliferation (Additional file 4: Fig. S4B), comparing with the parental cells. Remarkably, the existence of ABCC9 was induced in Dox-resistant MDA-MB-231 (MDA-MB-231/Dox) and MDA-MB-468 (MDA-MB-468/Dox) cells relative to MDA-MB-231 and MDA-MB-468 cells (Fig. 3A). The IC<sub>50</sub> value of Dox was reduced by the knockdown of ABCC9 in MDA-MB-231/Dox and MDA-MB-468/Dox cells (Fig. 3B and C). The numbers of Edu-positive MDA-MB-231/Dox and MDA-MB-468/Dox cells were attenuated by the depletion of ABCC9 (Fig. 3D). Meanwhile, the apoptosis of MDA-MB-231/Dox and MDA-MB-468/Dox cells was stimulated by the silencing of ABCC9 (Fig. 3E). consistently, the expression of cleaved caspase3 and cleaved caspase 9 was induced by the depletion of ABCC9 in the cells (Fig. 3F). Together these data imply that silencing of ABCC9 attenuates Dox resistance of BC cells.



### ZON attenuates Dox resistance of BC cells through inducing ferroptosis

Given that the ABCC9 was a potential oncogene according to the above results, we tried to explore the inhibitory agents targeting ABCC9 in BC cells. Previous studies have demonstrated the tumor inhibitory effect of ZON and we focused on the function of ZON in this study. The characterization of ZON was realized by using UV-visible spectrometry, FTIR spectroscopy, and SEM. The synthesized ZON nanoparticles exhibited an absorption peak at 350 nm (Additional file 5: Fig. S5A), which is consistent with previous report. Results from FTIR presented peaks at 882  $\text{cm}^{-1}$ , 1130  $\text{cm}^{-1}$ , 1460  $\text{cm}^{-1}$ , 1747  $\text{cm}^{-1}$ , 2854  $\text{cm}^{-1}$ , 2949  $\text{cm}^{-1}$ , and 3447  $\text{cm}^{-1}$ , which indicated C=C bending, C–O stretching, C–H bending, C=O stretching, C–H bond, alkane–CH stretching, and –OH stretching vibrations, respectively (Additional file 5: Fig S5B). Besides, Additional file 5: Fig S5C shows the SEM micrograph of synthesized ZnO nanoparticles. Next, we observed that the treatment of ZON decreased the IC<sub>50</sub> value of Dox in the suppression of MDA-MB-231/Dox and MDA-MB-468/Dox cell viability (Fig. 4A). Meanwhile, the treatment of ZON reduced the numbers of Edu-positive MDA-MB-231/Dox and MDA-MB-468/Dox cells (Fig. 4B). The apoptosis of MDA-MB-231/Dox and MDA-MB-468/Dox cells was induced by the treatment of ZON (Fig. 4C). Besides, given that previous study showed that ZON induced tumor suppressor function by activating p53, we validated the effect of ZON on p53 in BC cells. We confirmed that the total expression of p21, BAX, and nucleus accumulation of p53 were enhanced by the treatment of ZON in MDA-MB-231/Dox and MDA-MB-468/Dox cells (Fig. 4D).

Moreover, we found that treatment with erastin, a ferroptosis activator, led to suppressed viability and proliferation of Dox-resistant MDA-MB-231 (Additional file 6: Fig. S6A–C) and MDA-MB-468 cells (Additional file 6: Fig. S6D–F), compared with the control group. These data suggested that targeting ferroptosis can lead to the attenuation of doxorubicin resistance.

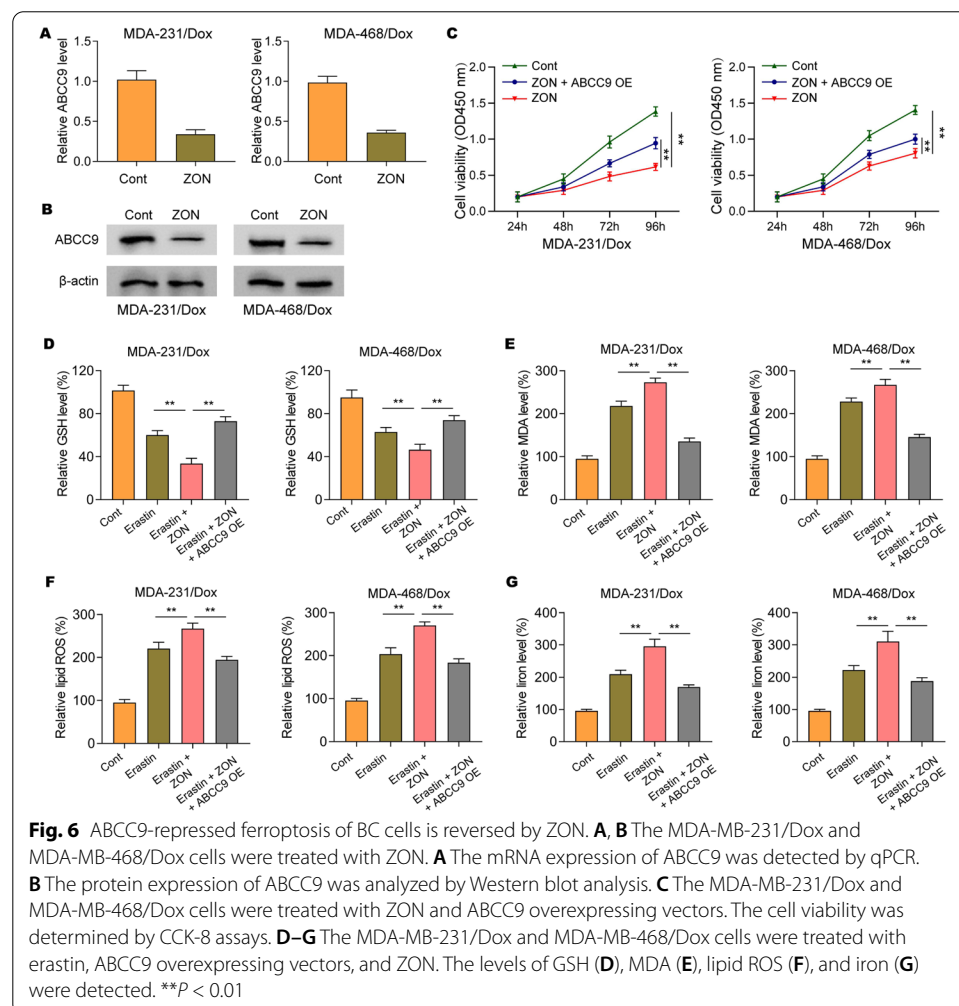


### ZON induces ferroptosis of BC cells by targeting p53

Given that p53 is a crucial ferroptosis regulator, we validated the correlation of ZON with p53 in the regulation of ferroptosis of BC cells. We observed that the treatment of erastin suppressed the cell viability of MDA-MB-231/Dox and MDA-MB-468/Dox cells and the treatment of ZON enhanced the phenotype (Fig. 5A and B). Meanwhile, the levels of GSH were reduced and the MDA, lipid ROS, and iron levels were enhanced by the treatment of erastin and the depletion of p53 could reverse the effect of erastin, while the co-treatment of ZON further reversed the effect of p53 depletion in MDA-MB-231/Dox and MDA-MB-468/Dox cells (Fig. 5C–F).

### ABCC9-repressed ferroptosis of BC cells is reversed by ZON

Next, we explored the correlation of ZON with ABCC9 in the modulation of ferroptosis of BC cells. We confirmed that the treatment of ZON remarkably repressed the expression of ABCC9 in MDA-MB-231/Dox and MDA-MB-468/Dox cells (Fig. 6A and B). ZON repressed the cell viability of MDA-MB-231/Dox and MDA-MB-468/Dox cells and the overexpression of ABCC9 reversed the repression (Fig. 6C). Moreover, the treatment of ZON reduced GSH levels and enhanced MDA, lipid ROS, and iron levels



in erastin-stimulated MDA-MB-231/Dox and MDA-MB-468/Dox cells, while the overexpression could reverse the effect of ZON (Fig. 6D–G). Moreover, although treatment with erastin and ZON induced ferroptosis, and suppressed the viability and proliferation of Dox-resistant cells, the overexpression of ABCC9 abolished these effects (Additional file 7: Fig. S7). Above results indicated that ABCC9 overexpression suppressed ferroptosis, possibly through p53 signaling.

### ZON attenuates tumor growth of BC cells by targeting ABCC9 in vivo

We then validated whether ZON regulated BC cell growth by targeting ABCC9 in vivo. The tumorigenicity analysis in xenograft model showed that the treatment of ZON attenuated the tumor growth of MDA-MB-231/Dox cells, while the overexpression of ABCC9 reversed the attenuation in the model (Fig. 7A and B). Meanwhile, we confirmed that the levels of Ki-67 and ABCC9 were repressed by ZON but the overexpression of ABCC9 could rescue the levels in the model (Fig. 7C and D).

### Discussion

BC is a prevalent gynecological cancer with high mortality and the chemotherapy resistance remains a huge clinical challenge for cure of BC. The mechanisms underlying chemoresistance are complicated and widely studied. These mechanisms include retarded transmembrane uptake of drugs via disrupting the function of influx drug transporters, enhancing activity of MDR efflux pumps of the ATP-binding cassette (ABC) superfamily including P-glycoprotein (ABCB1), multidrug resistance associated protein 1 (MRP1), and breast cancer resistance protein (ABCG2), as well as altered expression of drug targets, drug sequestration within organelles, metabolic drug inactivation, and antiapoptotic mechanisms (Amawi et al. 2019). P53 is a critical transcription factor that modulates the expression of multiple genes and responds to DNA damage, inducing cycle arrest or apoptosis (Sigal and Rotter 2000). It is reported that over half of human cancers

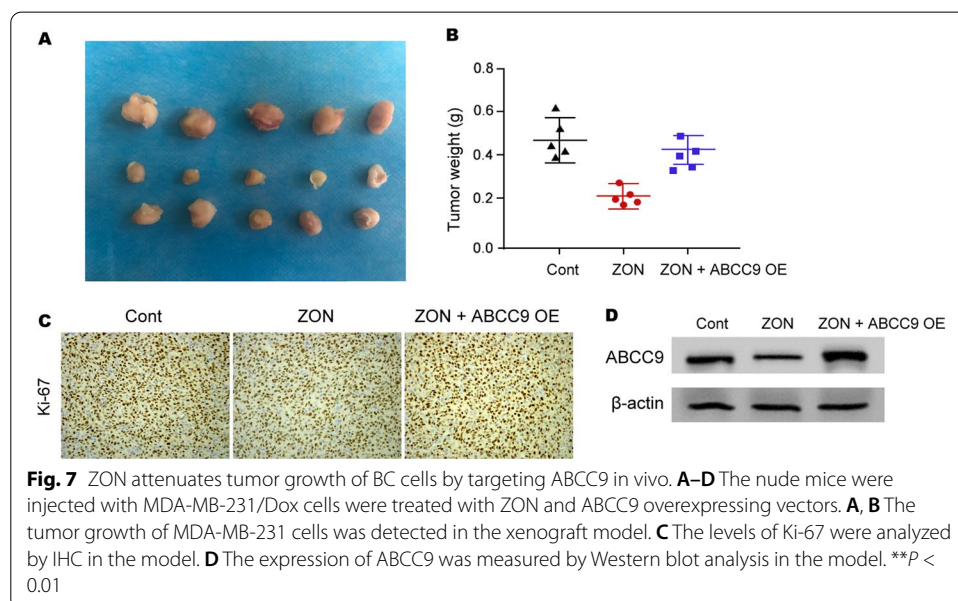


exhibit loss of function p53 mutation, which leads to impaired DNA binding, altered cell cycle progression, and apoptosis, and the consequent MDR (Sigal and Rotter 2000; Cao et al. 2020). Moreover, it is reported that p53 inhibits cystine uptake and sensitizes cells to ferroptosis upon reactive oxygen species (ROS)-induced stress, via repressing expression of SLC7A11 (Jiang et al. 2015). On the other hand, p53 promotes ferroptosis through enhancing expression of SAT1 (spermidine/spermine N1-acetyltransferase 1) and GLS2 (glutaminase 2) (Kang et al. 2019).

A recent study has reported that ABCC9 is upregulated in the clinical BC samples and functions as a potential diagnostic biomarker for BC patients (Zhang et al. 2020a, b), but the role of ABCC9 in BC is still elusive. In this work, we validated that ABCC9 was enhanced in clinical BC tissues and the high expression of ABCC9 was associated with a poor survival rate of BC patients and we identified the innovative function of ABCC9 in promoting Dox resistance and repressing ferroptosis of BC cells and discussed the inhibitory effect of ZONs on ABCC9.

The regulatory mechanisms of ferroptosis and Dox resistance in BC are complicated. FOXM1 regulates Dox resistance in BC by regulating DNA repair (Park et al. 2012). FSTL1 regulates stemness and chemoresistance in BC cells by integrin  $\beta$ 3/Wnt signaling (Cheng et al. 2019). Cytoprotective autophagy and BAG3 modulate Dox resistance in BC cells (Das et al. 2018). ACSL4 modulates ferroptosis by regulating cellular lipid composition in BC cells (Doll et al. 2017). GSK3 $\beta$ /Nrf2 signaling modulates erastin-stimulated ferroptosis in BC (Wu et al. 2020). Meanwhile, it has been reported that TRIM11 contributes to chemoresistance by the activation of  $\beta$ -catenin/ABCC9 signaling in nasopharyngeal carcinoma (Zhang et al. 2020a, b). ABCC9 is potential prognostic and diagnostic marker in BC (Zhang et al. 2020a, b). In the present work, we found that silencing of ABCC9 significantly repressed the proliferation, invasion/migration, and induced apoptosis of BC cells. Tumorigenicity analysis demonstrated that the tumor growth of BC cells was suppressed by the depletion of ABCC9 in the xenograft model of nude mice. Moreover, the treatment of ferroptosis activator erastin induced ferroptosis-related phenotypes and ABCC9 overexpression rescued the induction. The IC<sub>50</sub> value of Dox was reduced by the knockdown of ABCC9 in Dox-resistant BC cells (BC/Dox). The numbers of Edu-positive BC/Dox cells were attenuated by the depletion of ABCC9. Meanwhile, the apoptosis of BC/Dox cells was stimulated by the silencing of ABCC9. These data suggest that ABCC9 is a new contributor to BC progression. The clinical expression of ABCC9 and its correlation of ABCC9 with overall survival of BC should be validated by more studies. The potential agents targeted ABCC9 may be developed in the treatment of BC.

Moreover, the anti-tumor effect of ZONs in BC has been reported. ZONs induce apoptosis and oxidative stress in BC cells (Wahab et al. 2014). Chitosan-capped ZONs regulates apoptosis and cell cycle arrest by inducing p53 in BC cells (Anitha et al. 2019). Frizzled-7-targeted delivery of ZONs modulate drug resistance of BC cells (Ruenraroengsak et al. 2019). Our mechanical investigation showed that the treatment of ZONs attenuated Dox resistance of BC cells. ZONs remarkably repressed the expression of ABCC9 in BC/Dox cells. ZONs inhibited the cell viability of BC/Dox cells and the overexpression of ABCC9 reversed the repression. Moreover, the treatment of ZONs reduced GSH levels and enhanced MDA, lipid ROS, and iron levels in erastin-stimulated

BC/Dox cells, while the overexpression could reverse the effect of ZONs. The tumorigenicity analysis in xenograft model showed that the treatment of ZONs attenuated the tumor growth of BC/Dox cells, while the overexpression reversed the attenuation in the model. There were still some limitations in the current study. For example, the Deferoxamine or bathocuproine can be used to shown specific of the reaction. The clinical significance of ZONs should be explored in future investigations.

Our data indicate that ZONs are one of the potential candidates to inhibit ABCC9 in BC development. Our finding provides new molecular basic of the application of ZONs in the treatment of BC by targeting ABCC9. The relationship of the targets, such as ABCC9 and p53, of ZONs-inhibited cancer progression should be evaluated in further studies. We identified that ZONs could suppress the expression of ABCC9 and the overexpression of ABCC9 could reverse the effect of ZONs on BC/Dox cells. The mechanisms underlying ZONs-mediated ABCC9 need to be identified in future investigations.

## Conclusions

In conclusion, we discovered that the inhibition of ABCC9 by zinc oxide nanoparticles induces ferroptosis and attenuates Dox resistance in BC.

## Abbreviations

ZONs: Zinc oxide nanoparticles; BC: Breast cancer; Dox: Doxorubicin; BC/Dox: Dox-resistant BC cells.

## Supplementary Information

The online version contains supplementary material available at <https://doi.org/10.1186/s12645-021-00109-4>.

**Additional file 1: Fig. S1.** The expression of ABCC9 is elevated in clinical BC samples and associated with poor survival rate. (A) The expression of ABCC9 was analyzed by qPCR in clinical BC tissues ( $n = 152$ ) and adjacent non-tumor tissues ( $n = 152$ ). (B) The correlation of the expression of ABCC9 with overall survival of BC patients was analyzed.  $**P < 0.01$ . **Additional file 2: Fig. S2.** QRT-PCR assay to detect the level of ABCC9 mRNA in different breast cancer cell lines. **Additional file 3: Fig. S3.** Ferrostatin reverses ABCC9 depletion-induced ferroptosis of BC cells. (A-G) The MDA-MB-231 and MDA-MB-468 cells were treated with ABCC9 shRNA and ferrostatin (1 mmol/L). (A) The cell viability was determined by CCK-8 assays. (B) The cell proliferation was detected by Edu analysis. The levels of GSH (C), MDA (D), lipid ROS (E), and iron (F) were detected. (G) The expression of GPX4 and SLC7A11 was measured by Western blot analysis.  $**P < 0.01$ . **Additional file 4: Fig. S4.** Establishment of Dox-resistant breast cancer cell lines. MDA-MB-231, MDA-MB-468, MDA-MB-231/Dox, and MDA-MB-468/Dox cells were treated with Dox at indicated doses or 1  $\mu\text{g}/\text{mL}$ , then cell viability and proliferation were detected by CCK-8 and Edu assay. **Additional file 5: Fig. S5.** Characterization of ZON. The synthesized ZON were characterized by UV-VIS spectroscopy (A), Fourier Transform Infra-Red (FTIR) Spectroscopy (B), and Scanning electron microscopy (SEM) (C). **Additional file 6: Fig. S6.** ZON treatment inhibits viability and proliferation of Dox-resistant cell. The MDA-MB-231/Dox and MDA-MB-468/Dox cells were treated with erastin and ZON. The cell viability of MDA-MB-231/Dox (A and B) and MDA-MB-468/Dox (D and E) cells were determined by CCK-8 assay. The cell proliferation of MDA-MB-231/Dox (C) and MDA-MB-468/Dox (F) cells were determined by Edu assay. **Additional file 7: Fig. S7.** ABCC9 overexpression counteracts ZON-inhibited viability and proliferation of Dox-resistant cell. The MDA-MB-231/Dox and MDA-MB-468/Dox cells were transfected with ABCC9 overexpressing vectors, and treated with erastin and ZON. The cell viability of MDA-MB-231/Dox (A) and MDA-MB-468/Dox (C) cells were determined by CCK-8 assay. The cell proliferation of MDA-MB-231/Dox (B) and MDA-MB-468/Dox (D) cells were determined by Edu assay.

## Acknowledgements

Not applicable.

## Authors' contributions

YL, CJ, XZ and QZ designed the experiments. ZL and LC performed the experiments, SL and ST analyzed the data. YL, ZF and QZ wrote the paper. All authors read and approved the final manuscript.

## Funding

This study was supported by Supported by Natural Science Foundation of Liaoning Province, China (No. 2021-MS-070).

### Availability of data and materials

The datasets used and/or analyzed during the current study are available from the corresponding author on reasonable request.

### Declarations

#### Ethics approval and consent to participate

All experiments have acquired the consents of patients and were performed under approval of Cancer Hospital of China Medical University.

#### Consent for publication

Not applicable.

#### Competing interests

The authors declare that they have no competing interests.

#### Author details

<sup>1</sup>Department of Breast Surgery, Cancer Hospital of China Medical University, Liaoning Cancer Hospital & Institute, No. 44 Xiaoheyuan Road, Dadong District, Shenyang 110042, Liaoning Province, People's Republic of China. <sup>2</sup>Department of Medical Oncology, Cancer Hospital of China Medical University, Liaoning Cancer Hospital & Institute, No. 44 Xiaoheyuan Road, Dadong District, Shenyang 110042, Liaoning Province, People's Republic of China. <sup>3</sup>Department of Medical Imaging, Cancer Hospital of China Medical University, Liaoning Cancer Hospital & Institute, No. 44 Xiaoheyuan Road, Dadong District, Shenyang 110042, Liaoning Province, People's Republic of China. <sup>4</sup>Interventional Radiography Department, Affiliated Zhongshan Hospital of Dalian University, Dalian 116001, People's Republic of China. <sup>5</sup>Department of General Surgery, The Third People's Hospital of Dalian, Dalian Medical University, Dalian 116033, People's Republic of China.

Received: 15 October 2021 Accepted: 1 December 2021

Published online: 24 January 2022

### References

- Amawi H, Sim HM, Tiwari AK, Ambudkar SV, Shukla S (2019) ABC transporter-mediated multidrug-resistant cancer. *Adv Exp Med Biol* 1141:549–580
- Anitha J, Selvakumar R, Murugan K (2019) Chitosan capped ZnO nanoparticles with cell specific apoptosis induction through P53 activation and G2/M arrest in breast cancer cells - In vitro approaches. *Int J Biol Macromol* 136:686–696
- Cao X, Hou J, An Q, Assaraf YG, Wang X (2020) Towards the overcoming of anticancer drug resistance mediated by p53 mutations. *Drug Resist Updat* 49:100671
- Cheng S, Huang Y, Lou C, He Y, Zhang Y, Zhang Q (2019) FSTL1 enhances chemoresistance and maintains stemness in breast cancer cells via integrin beta3/Wnt signaling under miR-137 regulation. *Cancer Biol Ther* 20:328–337
- Dallavalle S, Dobricic V, Lazzarato L, Gazzano E, Machuqueiro M, Pajeva I et al (2020) Improvement of conventional anti-cancer drugs as new tools against multidrug resistant tumors. *Drug Resist Updat* 50:100682
- Das CK, Linder B, Bonn F, Rothweiler F, Dikic I, Michaelis M et al (2018) BAG3 overexpression and cytoprotective autophagy mediate apoptosis resistance in chemoresistant breast cancer cells. *Neoplasia* 20:263–279
- Dixon SJ, Lemberg KM, Lamprecht MR, Skouta R, Zaitsev EM, Gleason CE et al (2012) Ferroptosis: an iron-dependent form of nonapoptotic cell death. *Cell* 149:1060–1072
- Doll S, Proneth B, Tyurina YY, Panzilius E, Kobayashi S, Ingold I et al (2017) ACSL4 dictates ferroptosis sensitivity by shaping cellular lipid composition. *Nat Chem Biol* 13:91–98
- Elgendy SM, Alyammahi SK, Alhamad DW, Abdin SM, Omar HA (2020) Ferroptosis: an emerging approach for targeting cancer stem cells and drug resistance. *Crit Rev Oncol Hematol* 155:103095
- Harbeck N, Gnant M (2017) Breast cancer. *Lancet* 389:1134–1150
- Hu C, Du W (2020) Zinc oxide nanoparticles (ZnO NPs) combined with cisplatin and gemcitabine inhibits tumor activity of NSCLC cells. *Aging* 12:25767–25777
- Huang CC, Chia WT, Chung MF, Lin KJ, Hsiao CW, Jin C et al (2016) An implantable depot that can generate oxygen in situ for overcoming hypoxia-induced resistance to anticancer drugs in chemotherapy. *J Am Chem Soc* 138:5222–5225
- Jiang L, Kon N, Li T, Wang SJ, Su T, Hibshoosh H et al (2015) Ferroptosis as a p53-mediated activity during tumour suppression. *Nature* 520:57–62
- Kang R, Kroemer G, Tang D (2019) The tumor suppressor protein p53 and the ferroptosis network. *Free Radic Biol Med* 133:162–168
- Karagoz B, Suleymanoglu S, Uzun G, Bilgi O, Aydinov S, Haholu A et al (2008) Hyperbaric oxygen therapy does not potentiate doxorubicin-induced cardiotoxicity in rats. *Basic Clin Pharmacol Toxicol* 102:287–292
- Kathawala RJ, Gupta P, Ashby CR Jr, Chen ZS (2015) The modulation of ABC transporter-mediated multidrug resistance in cancer: a review of the past decade. *Drug Resist Updat* 18:1–17
- Li W, Zhang H, Assaraf YG, Zhao K, Xu X, Xie J et al (2016) Overcoming ABC transporter-mediated multidrug resistance: Molecular mechanisms and novel therapeutic drug strategies. *Drug Resist Updat* 27:14–29
- Liu J, Ma X, Jin S, Xue X, Zhang C, Wei T et al (2016) Zinc oxide nanoparticles as adjuvant to facilitate doxorubicin intracellular accumulation and visualize pH-responsive release for overcoming drug resistance. *Mol Pharm* 13:1723–1730
- Lu B, Chen XB, Ying MD, He QJ, Cao J, Yang B (2017) The role of ferroptosis in cancer development and treatment response. *Front Pharmacol* 8:992

- McGranahan N, Swanton C (2017) Clonal heterogeneity and tumor evolution: past, present, and the future. *Cell* 168:613–628
- Park YY, Jung SY, Jennings NB, Rodriguez-Aguayo C, Peng G, Lee SR et al (2012) FOXM1 mediates Dox resistance in breast cancer by enhancing DNA repair. *Carcinogenesis* 33:1843–1853
- Ruenraroengsak P, Kiryushko D, Theodorou IG, Klosowski MM, Taylor ER, Niriella T et al (2019) Frizzled-7-targeted delivery of zinc oxide nanoparticles to drug-resistant breast cancer cells. *Nanoscale* 11:12858–12870
- Siegel RL, Miller KD, Jemal A (2020) Cancer statistics, 2020. *CA Cancer J Clin* 70:7–30
- Sigal A, Rotter V (2000) Oncogenic mutations of the p53 tumor suppressor: the demons of the guardian of the genome. *Cancer Res* 60:6788–6793
- Steele A, Bayer I, Loth E (2009) Inherently superoleophobic nanocomposite coatings by spray atomization. *Nano Lett* 9:501–505
- Telli ML, Gradishar WJ, Ward JH (2019) NCCN guidelines updates: breast cancer. *J Natl Compr Canc Netw* 17:552–555
- Wahab R, Siddiqui MA, Saquib Q, Dwivedi S, Ahmad J, Musarrat J et al (2014) ZnO nanoparticles induced oxidative stress and apoptosis in HepG2 and MCF-7 cancer cells and their antibacterial activity. *Colloids Surf B Biointerfaces* 117:267–276
- Wang J, Lee JS, Kim D, Zhu L (2017) Exploration of zinc oxide nanoparticles as a multitarget and multifunctional anticancer nanomedicine. *ACS Appl Mater Interfaces* 9:39971–39984
- Wouters A, Pauwels B, Lardon F, Vermorken JB (2007) Review: implications of in vitro research on the effect of radiotherapy and chemotherapy under hypoxic conditions. *Oncologist* 12:690–712
- Wu X, Liu C, Li Z, Gai C, Ding D, Chen W et al (2020) Regulation of GSK3beta/Nrf2 signaling pathway modulated erastin-induced ferroptosis in breast cancer. *Mol Cell Biochem* 473:217–228
- Yagoda N, von Rechenberg M, Zaganjor E, Bauer AJ, Yang WS, Fridman DJ et al (2007) RAS-RAF-MEK-dependent oxidative cell death involving voltage-dependent anion channels. *Nature* 447:864–868
- Zhang R, Li SW, Liu L, Yang J, Huang G, Sang Y (2020a) TRIM11 facilitates chemoresistance in nasopharyngeal carcinoma by activating the beta-catenin/ABCC9 axis via p62-selective autophagic degradation of Daple. *Oncogenesis* 9:45
- Zhang X, Kang X, Jin L, Bai J, Zhang H, Liu W et al (2020b) ABCC9, NKAPL, and TMEM132C are potential diagnostic and prognostic markers in triple-negative breast cancer. *Cell Biol Int* 44:2002–2010

### Publisher's Note

Springer Nature remains neutral with regard to jurisdictional claims in published maps and institutional affiliations.

Ready to submit your research? Choose BMC and benefit from:

- fast, convenient online submission
- thorough peer review by experienced researchers in your field
- rapid publication on acceptance
- support for research data, including large and complex data types
- gold Open Access which fosters wider collaboration and increased citations
- maximum visibility for your research: over 100M website views per year

At BMC, research is always in progress.

Learn more [biomedcentral.com/submissions](https://biomedcentral.com/submissions)

